Ronn, John; Zhang, Jianhao; Zhang, Weiwei; Tu, Zhengrui; Matikainen, Antti; Leroux, Xavier; Duran-Valdeiglesias, Elena; Vulliet, Nathalie; Boeuf, Frederic; Alonso-Ramos, Carlos; Lipsanen, Harri; Vivien, Laurent; Sun, Zhipei; Cassan, Eric

Erbium-doped hybrid waveguide amplifiers with net optical gain on a fully industrial 300 mm silicon nitride photonic platform

Erbium-doped hybrid waveguide amplifiers with net optical gain on a fully industrial 300 mm silicon nitride photonic platform

JOHN RÖNN,[1,7,8] JIANHAO ZHANG,[2,7] WEIWEI ZHANG,[2,3]
ZHENGRUI TU,[2] ANTTI MATIKAINEN,[4] XAVIER LEROUX,[2] ELENA
DURÁN-VALDEIGLESIAS,[2] NATHALIE VULLIET,[5] FREDERIC BOEUF,[5]
CARLOS ALONSO-RAMOS,[2] HARRI LIPSANEN,[4] LAURENT VIVIEN,[2]
ZHIPEI SUN,[4,6,9] AND ERIC CASSAN[2,10]

[1]*Department of Neuroscience and Biomedical Engineering, Aalto University School of Science, Espoo, Finland*
[2]*Centre for Nanoscience and Nanotechnologies, Université Paris-Sud, Paris, France*
[3]*Optoelectronics Research Centre, University of Southampton, Southampton, UK*
[4]*Department of Electronics and Nanoengineering, Aalto University School of Electrical Engineering, Espoo, Finland*
[5]*STMicroelectronics, Silicon Technology Development, Crolles, France*
[6]*QTF Centre of Excellence, Department of Applied Physics, Aalto University School of Science, Espoo, Finland*
[7]*Contributed equally to this work*
[8]*john.ronn@aalto.fi*
[9]*zhipei.sun@aalto.fi*
[10]*eric.cassan@u-psud.fr*

Abstract: Recently, erbium-doped integrated waveguide devices have been extensively studied as a CMOS-compatible and stable solution for optical amplification and lasing on the silicon photonic platform. However, erbium-doped waveguide technology still remains relatively immature when it comes to the production of competitive building blocks for the silicon photonics industry. Therefore, further progress is critical in this field to answer the industry's demand for infrared active materials that are not only CMOS-compatible and efficient, but also inexpensive and scalable in terms of large volume production. In this work, we present a novel and simple fabrication method to form cost-effective erbium-doped waveguide amplifiers on silicon. With a single and straightforward active layer deposition, we convert passive silicon nitride strip waveguide channels on a fully industrial 300 mm photonic platform into active waveguide amplifiers. We show net optical gain over sub-cm long waveguide channels that also include grating couplers and mode transition tapers, ultimately demonstrating tremendous progress in developing cost-effective active building blocks on the silicon photonic platform.

1. Introduction

Modern information society is based on a physical infrastructure where electronics plays an essential role. Apart from low-loss optical fiber transmission channels, information processing occurs mainly via electronic routing and switching elements. Data centers, in particular, contain a very large number of electronic equipment and boards. Optical interconnects, in the form of transceivers, are seeing their development accelerate, particularly to cope with the increasing information bit rates and substantial power consumption in data centers [1]. For this reason, photonic integration has made a considerable progress over the recent years. However, among its main disadvantages, the indirect nature of the silicon's band structure, which prevents it from

emitting and amplifying optical signals, is the most critical. This has led to severe challenges in developing solutions for on-chip optical amplification and lasing without having to resort to energy expensive optical/electronic conversions. In this context, the hetero-integration of III/V semiconductor amplifiers on silicon, as developed recently, is a possible answer but still remains complex and expensive in terms of fabrication and all-monolithic integration [2]. On the other hand, a much simpler and inexpensive solution has been proposed for years. It consists of reproducing the operation principle of all-optical erbium-doped fiber amplifiers (EDFA) [3] into the form of erbium-doped integrated waveguide amplifiers (EDWA) [4]. Indeed, such devices have been recently explored to develop some of the essential active functionalities on the silicon photonic platform where cost-effective mass production methods for CMOS-compatible amplifier and laser devices are highly desired [5,6].

However, the transition from EDFAs to fully integrated silicon-compatible EDWAs is not trivial. The greatest challenge comes from the typical active waveguide lengths that usually scale in hundreds of µm in photonic integrated circuits instead of several tens of meters for optical fibers. Moreover, light propagation losses in sub-µm^2 (or even narrower) cross-section waveguides are usually few dB/cm while fiber losses can be five orders of magnitude lower at 1.55 µm. The dramatic reduction in the amplification lengths combined with the strong increase in the optical losses imply that tremendous efforts need to be made not only on the active material quality, but also for the optimization of the waveguide passive losses. These challenges are, in fact, anything but obvious and constitute difficult issues to resolve. One of the accessible solutions is to increase the erbium-ion doping level and, thus, the optical gain per unit length provided by the active waveguide in order to compensate the considerable waveguide losses. Yet, the erbium-doping can be increased up to a certain limit as the high erbium-incorporation introduces unwanted transitions and quenching of active ions within the gain medium, which ultimately lead to diminishing returns in the amplifier performance. To optimize the performance of erbium-based integrated amplifier devices, various host materials and different fabrication methods have been studied to achieve high erbium-incorporation inside different compounds [7–19]. Additionally, unique waveguide geometries have also been proposed to maximize the interaction of the guided beams with the active layer [20–25]. Despite the recent progress in the field, there is still a relatively long way to go before erbium-based integrated devices can be established as fundamental active building blocks in the silicon photonics industry. Further improvements, such as higher gain, scalable fabrication process and lower deposition temperatures need to be pursued for ultimate cost-efficiency and silicon photonic circuit compatibility.

In this work, we present a simple and cost-effective method to fabricate erbium-doped integrated waveguide amplifiers on silicon by combining a fully industrial 300 mm silicon nitride photonic platform with a scalable and CMOS-compatible atomic layer deposition process. On this photonic platform, we use the simplest form of waveguides, i.e. silicon nitride strip waveguides in order to produce waveguide amplifiers with small cross-sections. We also study various doping levels of erbium and show that internal net optical gain can be produced over sub-cm long waveguide channels that also include grating couplers and mode transition tapers. Ultimately, the results and methods presented in this work show significant progress in developing cost-effective integrated waveguide amplifiers on silicon, thus, opening a solid path to the future realization of silicon-erbium-based micro-cavity and multi-channel laser devices where optical gain achieved in compact footprint is highly desired.

2. Experimental details

2.1. Device fabrication

In this work, erbium-doped hybrid waveguide amplifiers were fabricated as follows. Firstly, passive silicon nitride waveguide channels were produced by depositing optical-quality silicon dioxide (thickness: 1.4 µm) and silicon nitride (thickness: 600 nm) layers on a 300 mm silicon

wafer by low-pressure and plasma-enhanced chemical vapor depositions, respectively, followed by deep-ultraviolet lithography (248 nm) and reactive ion etching. The fabrication process was then completed by coating the passive waveguide channels with a ~150 nm thick layer of erbium-doped alumina (Er:Al$_2$O$_3$) by sequentially depositing erbium oxide (Er$_2$O$_3$) and aluminum oxide (Al$_2$O$_3$) onto the surface of the waveguides with thermal ALD (Beneq TFS-500). The erbium oxide was grown with Er(thd)$_3$ and ozone precursors, whereas the aluminum oxide was grown with trimethylaluminum (TMA) and water precursors. Four different film compositions were deposited at 300 °C by varying the relative Er$_2$O$_3$/Al$_2$O$_3$ supercycle sequence for each process. The cycle sequences and the resulting film compositions of the layers are presented in Table 1. The elemental compositions were measured from planar reference samples with energy-dispersive X-ray spectroscopy by focusing a high-energy beam (15 keV) of electrons onto each sample while recording their characteristic X-ray spectra. The samples were found to be slightly oxygen rich with Er-concentrations ranging from 1.11 to 3.88 at.% (equivalent to $1.11 - 3.88 \cdot 10^{21}$ cm^{-3} of Er-ions in amorphous Al$_2$O$_3$).

Figure 1 presents a schematic view of the designed waveguide amplifier structure. Each amplifier channel contains one single-mode strip waveguide (width: 400 nm, height: 600 nm, length: 100–2000 µm), preceded and followed by grating couplers (width: 15 µm, height: 600 nm, length: 100 µm) and multi-mode to single-mode transition tapers (height: 600 nm, length: 500 µm) at the input and output sides of the corresponding channel, as illustrated in Fig. 1(a). Fiber-to-waveguide coupling is achieved with the input and output grating couplers (coupling efficiency for each side: -10/-14 dB at 1480/1533 nm, 3 dB bandwidth: ~50 nm at 1480 nm). Once coupled, the optical beam is guided to the multi-mode to single-mode transition taper that converts the beam suitable for the single-mode strip waveguide. When combined with the Er:Al$_2$O$_3$ active layer, the waveguide channel can act as an integrated optical amplifier. To eliminate leaky losses in the waveguides, a layer of PMMA-resist was spin-coated onto each device to achieve vertically-quasi-symmetric mode confinement. Figure 1(b) shows the simplified cross-section at the central axis of the fabricated waveguide amplifiers as well as the electric field distributions ($|\mathbf{E}_{x/y}|^2$) of the fundamental transverse modes (TE/TM) propagating at the corresponding cross-section at $\lambda = 1533$ nm. In this work, we operate the waveguide amplifiers by coupling only the fundamental TE-modes of the pump and signal beams into the devices.
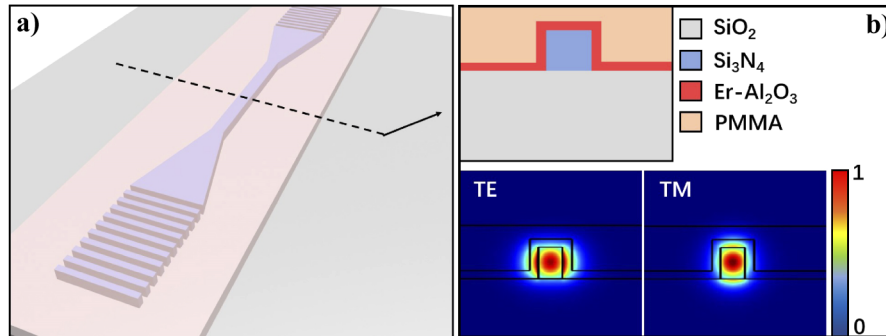
Fig. 1. Schematic illustration of the Er:Al$_2$O$_3$–Si$_3$N$_4$ waveguide amplifier structure. a) Layout of the waveguide amplifier circuit; b) Simplified cross-section at the central axis of the waveguide amplifier as well as the electric field distributions ($|\mathbf{E}_{x/y}|^2$) of the fundamental transverse modes (TE/TM) propagating at the corresponding cross-section at $\lambda = 1533$ nm.

Table 1. Properties and preparation conditions of the Er:Al$_2$O$_3$ active layers.

Layer	Number of cycles			Thickness (nm)	Elemental composition (at.%)		
	Er$_2$O$_3$	Al$_2$O$_3$	Total		O	Al	Er
1	1	12	125	146.6	64.26	34.63	1.11
2	1	6	250	149.8	63.53	34.49	1.98
3	1	3	500	150.6	63.28	33.64	3.08
4	1	2	750	151.1	62.92	33.20	3.88

2.2. Device characterization

The transmission and amplification properties of the fabricated waveguide amplifiers were characterized via a conventional grating-coupling measurement setup. A high-power laser operating at 1480 nm was used as the pump source, whereas a tunable laser operating at 1533 nm was used as the signal laser. The high-power pump laser was combined with the signal laser and then transmitted through a 2-2 power splitter (90/10 %). The polarization state of the signal laser was controlled with a manual polarization controller. The power from the 10 % port was connected with an attenuator and a power-meter for power recording, while another output was guided into the integrated waveguide through a grating coupler. The power of the coupled signal beam was set approximately to 1 µW and the output power from the waveguide was collected with an optical spectrum analyzer for optical gain monitoring. By using a tunable attenuator, the launched pump power was tuned from -30 dBm to 16 dBm discretely with sufficient dwell time for accurate data acquisition. At each power level, the signal enhancement at the signal wavelength was measured and double-checked by the difference between the pump-on and pump-off states. The background noise of the pump source was found negligible in both signal-off and signal-on states. The noise at the signal wavelength was measured in the signal-off state and turned out to be no more than -50 dBm. The collected signal power was obtained by subtracting the pump-induced noise and amplified spontaneous emission from the signal peak power. The internal modal gain (g_{mod}) generated in the waveguide amplifier was then calculated via

$$g_{\text{mod}}[\text{dB/cm}] = \frac{10}{L}\log_{10}\left(\frac{S_{\text{Pump on}}[\text{W}] - \text{ASE}[\text{W}]}{S_{\text{Pump off}}[\text{W}]}\right) - \alpha, \qquad (1)$$

where L is the waveguide length (in cm) $S_{\text{Pump on}}$ and $S_{\text{Pump off}}$ the measured signal powers in the presence and absence of pumping, respectively, ASE the measured power resulting from amplified spontaneous emission and α the total propagation loss of the waveguide (in dB/cm) in the absence of pumping.

3. Results and discussion

3.1. Transmission measurements

The transmission properties of the fabricated waveguide amplifiers were studied via the well-known cutback method [26] by coupling only the signal beam (λ_c = 1533 nm, P_{in} = 100 nW) into waveguide amplifier channels of varying lengths. Figure 2(a) presents the relative propagation loss of the signal beam after having propagated in 1.2, 1.6, 2.1 and 3.1 mm long waveguide amplifiers in the absence of the pump beam.The transmission data is shown as solid points for each individual waveguide amplifier (i.e. length and active layer). The total propagation loss of each waveguide amplifier set was then determined by linear least-squares fitting, as shown by the solid lines in Fig. 2(a). The evaluated total propagation loss values are given in Table 2 and shown in Fig. 2(b) as a function of the active layer erbium-concentration (solid points). It is worthwhile to note that the evaluated total propagation loss equals to loss occurring in the single-mode

waveguides of the corresponding waveguide channels since only the length of the single-mode waveguide varies in our waveguide amplifier design. As such, the total propagation loss occurring in the single-mode waveguides can be related to the active layer erbium-concentration via

$$\alpha_{sm}(N_0)\,[\text{dB/cm}] = \alpha_0 + 10\log_{10}(e)\sigma_{12}\Gamma_{sm}N_0, \qquad (2)$$

where σ_{12} is the absorption cross-section of erbium at the signal wavelength (1533 nm), Γ_{sm} the mode confinement factor of the signal beam with the active region of the waveguide amplifier for the single-mode cross-section and α_0 the passive propagation loss of the waveguide (i.e. scattering loss). Now, by applying a linear least-squares fit to the total propagation loss data, we can determine the values for α_0 and σ_{12}. Since Γ_{sm} equals to 0.317 at 1533 nm, best fit is obtained with $\sigma_{12} = 5.698 \pm 0.316 \times 10^{-21}$ cm^2 and $\alpha_0 = 1.912 \pm 0.342$ dB/cm. The evaluated value for the absorption cross-section coincides with the one found in the literature for Er:Al$_2$O$_3$ [4] and the order of the passive propagation loss is close to what should be expected from the waveguides. Finally, we evaluate the total propagation loss occurring over the entire (unpumped) waveguide channels via

$$\alpha_{tot}(\text{dB}) = L_{sm}\alpha_{sm} + 2L_{mm}\alpha_{sm}\frac{\Gamma_{mm}}{\Gamma_{sm}} + 2L_{tt}\alpha_{sm}\frac{\Gamma_{tt}}{\Gamma_{sm}}, \qquad (3)$$

where L_{sm}, L_{mm} and L_{tt} are the lengths of the single-mode waveguide, multi-mode waveguide and transition taper in the corresponding waveguide channel, respectively, and Γ_{mm} and Γ_{tt} the mode confinement factors for the multi-mode waveguide and transition taper, respectively. As such, the loss is calculated for each section in the waveguide channel separately. Since the value of Γ_{tt} is not constant throughout the channel, but instead varies between $0.06 - 0.13$, an average value of $\Gamma_{tt} \approx 0.095$ was assumed, which can be justified due to the linear nature of the multi-mode to single-mode transition taper. The calculated propagation loss values for the studied waveguide amplifiers are listed in Table 2.
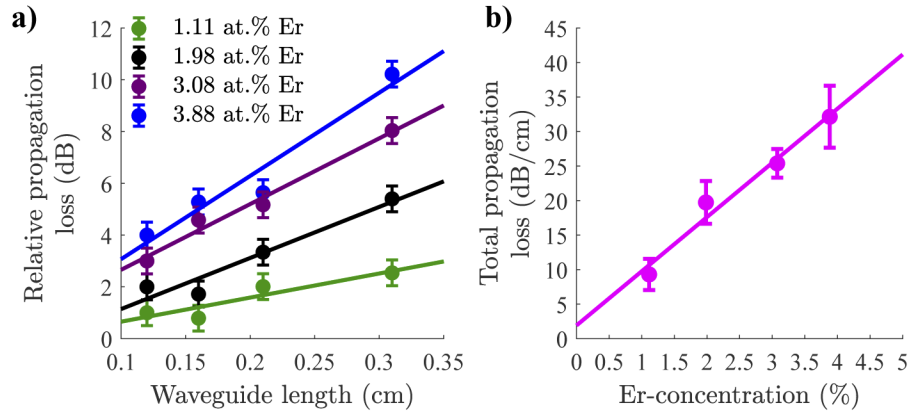
Fig. 2. Transmission characterization of the Er:Al$_2$O$_3$–Si$_3$N$_4$ waveguide amplifiers. a) Relative propagation loss of the signal beam ($\lambda_c = 1533$ nm, $P_{in} = 100$ nW) after having propagated in 1.2, 1.6, 2.1 and 3.1 mm long waveguide amplifiers in the absence of the pump beam; b) Evaluated total propagation loss for the single-mode cross-section at 1533 nm as a function of the erbium-concentration. In a) each data set has been shifted for clarity.

3.2. Gain measurements

The amplification properties of the fabricated waveguide amplifiers were studied by co-coupling the signal ($\lambda_c = 1533$ nm, $P_{in} = 1$ µW) and pump ($\lambda_c = 1480$ nm, $P_{in} = 0 - 18$ mW) beams

Table 2. Measured transmission and amplification properties of the studied Er:Al$_2$O$_3$–Si$_3$N$_4$ waveguide amplifiers.

Layer	α_{tot} [1.2/1.6 mm] (dB)	SE_{max} [1.2/1.6 mm] ($\pm$0.15 dB)	g_{mod} [1.2/1.6 mm] (dB/cm)
1	0.41 ± 0.10 / 0.78 ± 0.19	0.54 / 1.00	1.07 ± 1.50 / 1.35 ± 1.13
2	0.87 ± 0.14 / 1.66 ± 0.26	1.00 / 1.96	1.10 ± 1.69 / 1.85 ± 1.27
3	1.11 ± 0.09 / 2.13 ± 0.17	1.43 / 2.48	2.63 ± 1.46 / 2.20 ± 1.10
4	1.42 ± 0.20 / 2.70 ± 0.38	1.76 / 3.13	2.82 ± 2.07 / 2.65 ± 1.55

inside the waveguide amplifier channels. The signal enhancement generated by each waveguide amplifier was then measured by varying the launched pump power in progressive steps from 0 to 18 mW. The obtained results are presented in Figs. 3(a) and 3(b) for waveguide amplifier channels with lengths of 1.2 mm and 1.6 mm, respectively.Figs. 3(a) and 3(b) demonstrate that the signal enhancement generated by each waveguide amplifier increases as the erbium-concentration in the active layer is increased with saturation-like behaviour starting to occur after approximately 5 − 10 mW pump power is launched into the waveguide channels. To calculate the internal net modal gain generated by each waveguide amplifier, Eq. (1) was applied and the evaluated modal gain values are listed in Table 2. The highest net modal gain was obtained in the 1.2 mm long waveguide amplifier with active layer 4, whereas the lowest net modal gain was obtained in the 1.2 mm long waveguide amplifier with active layer 1. We also attempted to produce internal modal gain in the longer waveguide amplifiers (2.1 mm and 3.1 mm) but did not succeed as the maximum pump power used in this work was insufficient to induce gain saturation in the corresponding waveguide channels Therefore, further characterization with higher pumping conditions are necessary to extend and to optimize the overall gain of our proposed waveguide amplifiers.
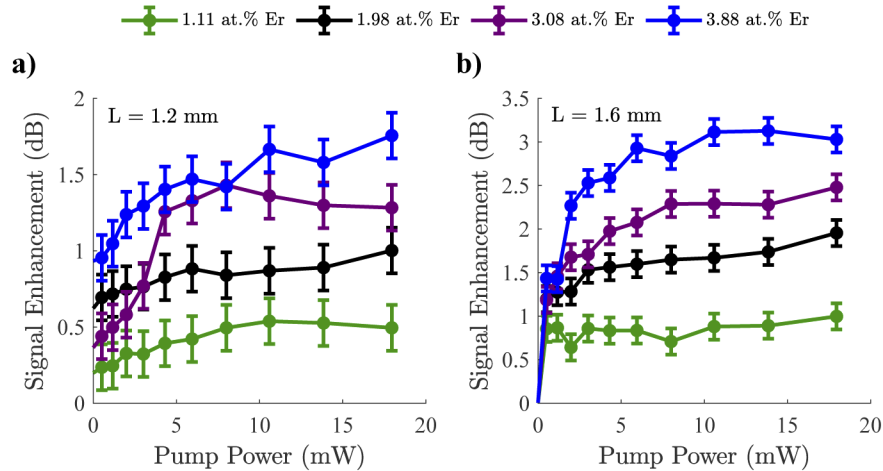
Fig. 3. Gain characterization of the Er:Al$_2$O$_3$–Si$_3$N$_4$ waveguide amplifiers. Signal enhancement generated by a) the 1.2 mm long and b) the 1.6 mm long waveguide amplifier for a signal beam with λ_c = 1533 nm and $P_{in} \approx$ 1 μW as a function of the launched pump power (λ_c = 1480 nm, P_{in} = 0 − 18 mW).

In conclusion, this work demonstrates the simplicity of producing erbium-doped waveguide amplifiers with internal net optical gain on silicon. The hybrid waveguide amplifier concept demonstrated in this work can be further adapted to silicon waveguides since the pumping of the active waveguide channels was conducted at 1480 nm (instead of at 980 nm) where silicon

shows great transparency. The proximity of the pump wavelength to the signal wavelength also enables the use and design of single grating couplers for the light injection/extraction from/into the coupling fibers, which further simplifies the circuit design and reduces processing costs. Ultimately, the amplifier configuration proposed in this work combines simplicity, broad compatibility with the CMOS-technology, and demonstrates a method to amplify the data- and telecom signals with a standard pump laser source delivering only a few milliwatts of optical power.

4. Summary

As a summary, we present a novel and straightforward fabrication method to produce Er-doped integrated waveguide amplifiers on silicon with cost-effective methods. With a single active layer deposition, we convert passive silicon nitride strip waveguides into active waveguide amplifiers that exhibit internal net modal gain. Ultimately, this work shows significant advances towards optical amplification on a silicon chip with all the benefits supporting mass development of optical functions for integrated circuits.

Disclosures

The authors declare no conflicts of interest.

References

1. A. M. Urbas, Z. Jacob, L. Dal, D. Thomson, A. Zilkie, J. E. Bowers, and T. Komljenovic, "Roadmap on silicon photonics," J. Opt. **18**(7), 073003 (2016).
2. G.-H. Duan, C. Jany, A. Le Liepvre, A. Accard, M. Lamponi, D. Make, P. Kaspar, G. Levaufre, N. Girard, F. Lelarge, J.-M. Fedeli, A. Descos, B. B. Bakir, S. Messaoudene, D. Bordel, S. Menezo, G. de Valicourt, S. Keyvaninia, G. Roelkens, D. van Thourhout, D. J. Thomson, F. Y. Gardes, and G. T. Reed, "Hybrid iii–v on silicon lasers for photonic integrated circuits on silicon," IEEE J. Sel. Top. Quantum Electron. **20**(4), 158–170 (2014).
3. E. Desurvire, C. R. Giles, J. R. Simpson, and J. L. Zyskind, "Erbium-doped fiber amplifier," (1991). US Patent 5,005,175.
4. J. D. Bradley and M. Pollnau, "Erbium-doped integrated waveguide amplifiers and lasers," Laser Photonics Rev. **5**(3), 368–403 (2011).
5. J. D. Bradley and E. S. Hosseini, "Monolithic erbium-and ytterbium-doped microring lasers on silicon chips," Opt. Express **22**(10), 12226–12237 (2014).
6. M. Pollnau and J. D. Bradley, "Optically pumped rare-earth-doped al_2o_3 distributed-feedback lasers on silicon," Opt. Express **26**(18), 24164–24189 (2018).
7. G. N. van den Hoven, E. Snoeks, A. Polman, J. W. M. van Uffelen, Y. S. Oei, and M. K. Smit, "Photoluminescence characterization of Er?implanted Al_2O_3 films," Appl. Phys. Lett. **62**(24), 3065–3067 (1993).
8. M. P. Hehlen, N. J. Cockroft, T. R. Gosnell, A. J. Bruce, G. Nykolak, and J. Shmulovich, "Uniform upconversion in high-concentration Er^{3+}-doped soda lime silicate and aluminosilicate glasses," Opt. Lett. **22**(11), 772–774 (1997).
9. F. D. Patel, S. DiCarolis, P. Lum, S. Venkatesh, and J. N. Miller, "A compact high-performance optical waveguide amplifier," IEEE Photonics Technol. Lett. **16**(12), 2607–2609 (2004).
10. H. Isshiki, M. J. De Dood, A. Polman, and T. Kimura, "Self-assembled infrared-luminescent Er-Si-O crystallites on silicon," Appl. Phys. Lett. **85**(19), 4343–4345 (2004).
11. T. T. Van and J. P. Chang, "Controlled erbium incorporation and photoluminescence of er-doped y_2o_3," Appl. Phys. Lett. **87**(1), 011907 (2005).

12. X. Qiao, X. Fan, and M. Wang, "Luminescence behavior of Er^{3+} in glass ceramics containing BaF_2 nanocrystals," Scr. Mater. **55**(3), 211–214 (2006).

13. A. Kahn, H. Kühn, S. Heinrich, K. Petermann, J. D. Bradley, K. Wörhoff, M. Pollnau, Y. Kuzminykh, and G. Huber, "Amplification in epitaxially grown $Er:(Gd,Lu)_2O_3$ waveguides for active integrated optical devices," J. Opt. Soc. Am. B **25**(11), 1850–1853 (2008).

14. K. Wörhoff, J. D. Bradley, F. Ay, D. Geskus, T. Blauwendraat, and M. Pollnau, "Reliable Low-Cost Fabrication of Low-Loss $Al_2O_3:Er^{3+}$ Waveguides With 5.4-dB Optical Gain," IEEE J. Quantum Electron. **45**(5), 454–461 (2009).

15. R. R. Thomson, N. D. Psaila, S. J. Beecher, and A. K. Kar, "Ultrafast laser inscription of a high-gain Er-doped bismuthate glass waveguide amplifier," Opt. Express **18**(12), 13212–13219 (2010).

16. J. Rönn, L. Karvonen, C. J. Kauppinen, A. P. Perros, N. Peyghambarian, H. Lipsanen, A. Saynatjoki, and Z. Sun, "Atomic layer engineering of Er-ion distribution in highly doped $Er:Al_2O_3$ for photoluminescence enhancement," ACS Photonics **3**(11), 2040–2048 (2016).

17. D. Brüske, S. Suntsov, C. E. Rüter, and D. Kip, "Efficient ridge waveguide amplifiers and lasers in Er-doped lithium niobate by optical grade dicing and three-side Er and Ti in-diffusion," Opt. Express **25**(23), 29374–29379 (2017).

18. S. A. Vázquez-Córdova, S. Aravazhi, C. Grivas, Y.-S. Yong, S. M. García-Blanco, J. L. Herek, and M. Pollnau, "High optical gain in erbium-doped potassium double tungstate channel waveguide amplifiers," Opt. Express **26**(5), 6260–6266 (2018).

19. P. Q. Zhou, X. J. Wang, Y. D. He, Z. F. Wu, J. L. Du, and E. G. Fu, "Effect of deposition mechanisms on the infrared photoluminescence of erbium-ytterbium silicate films under different sputtering methods," J. Appl. Phys. **125**(17), 175114 (2019).

20. G. Van den Hoven, R. Koper, A. Polman, C. Van Dam, J. Van Uffelen, and M. Smit, "Net optical gain at 1.53 μm in er-doped al₂o₃ waveguides on silicon," Appl. Phys. Lett. **68**(14), 1886–1888 (1996).

21. R. Guo, X. Wang, K. Zang, B. Wang, L. Wang, L. Gao, and Z. Zhou, "Optical amplification in Er/Yb silicate strip loaded waveguide," Appl. Phys. Lett. **99**(16), 161115 (2011).

22. E. S. Hosseini, J. D. Bradley, J. Sun, G. Leake, T. N. Adam, D. D. Coolbaugh, and M. R. Watts, "Cmos-compatible 75 mw erbium-doped distributed feedback laser," Opt. Lett. **39**(11), 3106–3109 (2014).

23. X. J. Wang, L. J. Jiang, R. M. Guo, R. Ye, and Z. P. Zhou, "Spontaneous emission rate and optical amplification of Er3+ in double slot waveguide," Sci. China Math. **58**(10), 1–14 (2015).

24. J. Rönn, W. Zhang, A. Autere, X. Leroux, L. Pakarinen, C. Alonso-Ramos, A. Säynätjoki, H. Lipsanen, L. Vivien, E. Cassan, and Z. Sun, "Ultra-high on-chip optical gain in erbium-based hybrid slot waveguides," Nat. Commun. **10**(1), 432 (2019).

25. H. C. Frankis, H. M. Mbonde, D. B. Bonneville, C. Zhang, R. Mateman, A. Leinse, and J. D. Bradley, "Erbium-doped teo₂-coated si₃n₄ waveguide amplifiers with 5 db net gain," Photonics Res. **8**(2), 127–134 (2020).

26. Y. Okamura, S. Yoshinaka, and S. Yamamoto, "Measuring mode propagation losses of integrated optical waveguides: a simple method," Appl. Opt. **22**(23), 3892–3894 (1983).